OMTN, Volume *35*

Supplemental information

Correction of human nonsense mutation via adenine base editing for Duchenne muscular dystrophy treatment in mouse

Ming Jin, Jiajia Lin, Haisen Li, Zhifang Li, Dong Yang, Yin Wang, Yuyang Yu, Zhurui Shao, Long Chen, Zhiqiang Wang, Yu Zhang, Xiumei Zhang, Ning Wang, Chunlong Xu, Hui Yang, Wan-Jin Chen, and Guoling Li

Supplemental Figure legend

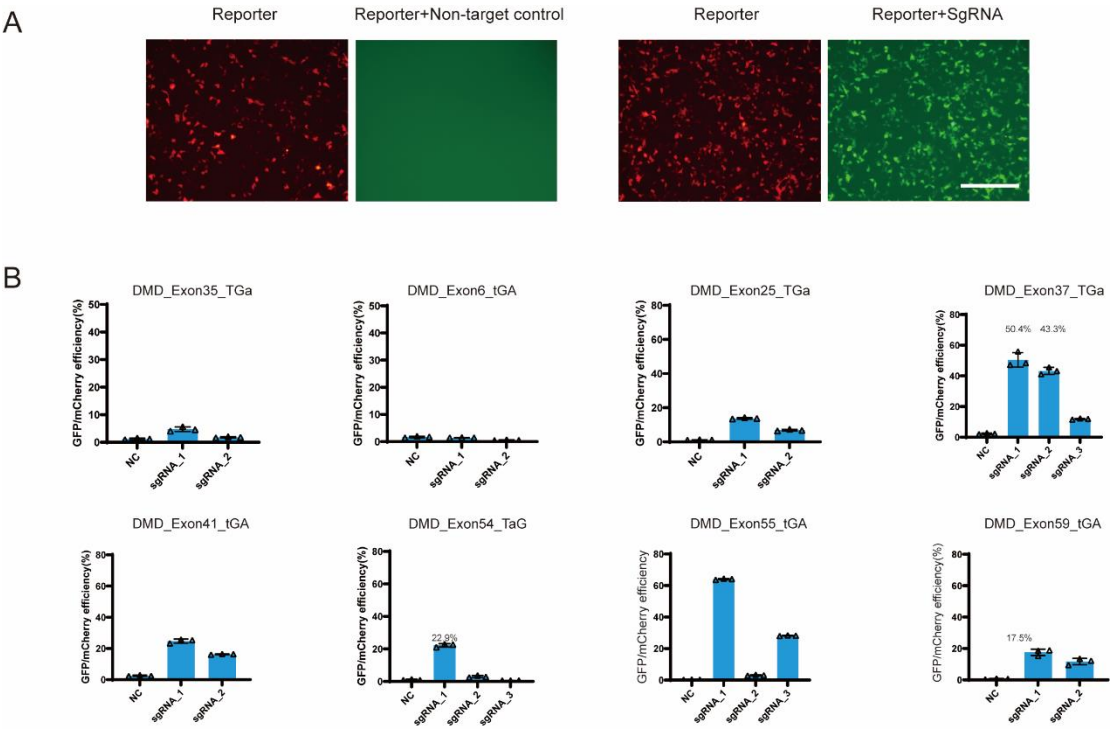

Figure S1. The efficiency of ABE and human sgRNAs in correcting nonsense mutations *in vitro.*

(A) Representative fluorescence microscopy pictures of mCherry and EGFP expressions in HEK293T cells after transfection of the reporter plasmid alone or its combination with ABE construct. Scale bar, 200 μm. **(B)** FACS detection of EGFP expression levels in HEK293T cells treated with SpG-ABE and sgRNAs targeting human exon 4, 6, 21, 25, 35, 37, 41, 54, 55, and 59 (n=3). Quantification is present as mean ± SEM. *P < 0.05; **P < 0.01; ***P < 0.001.

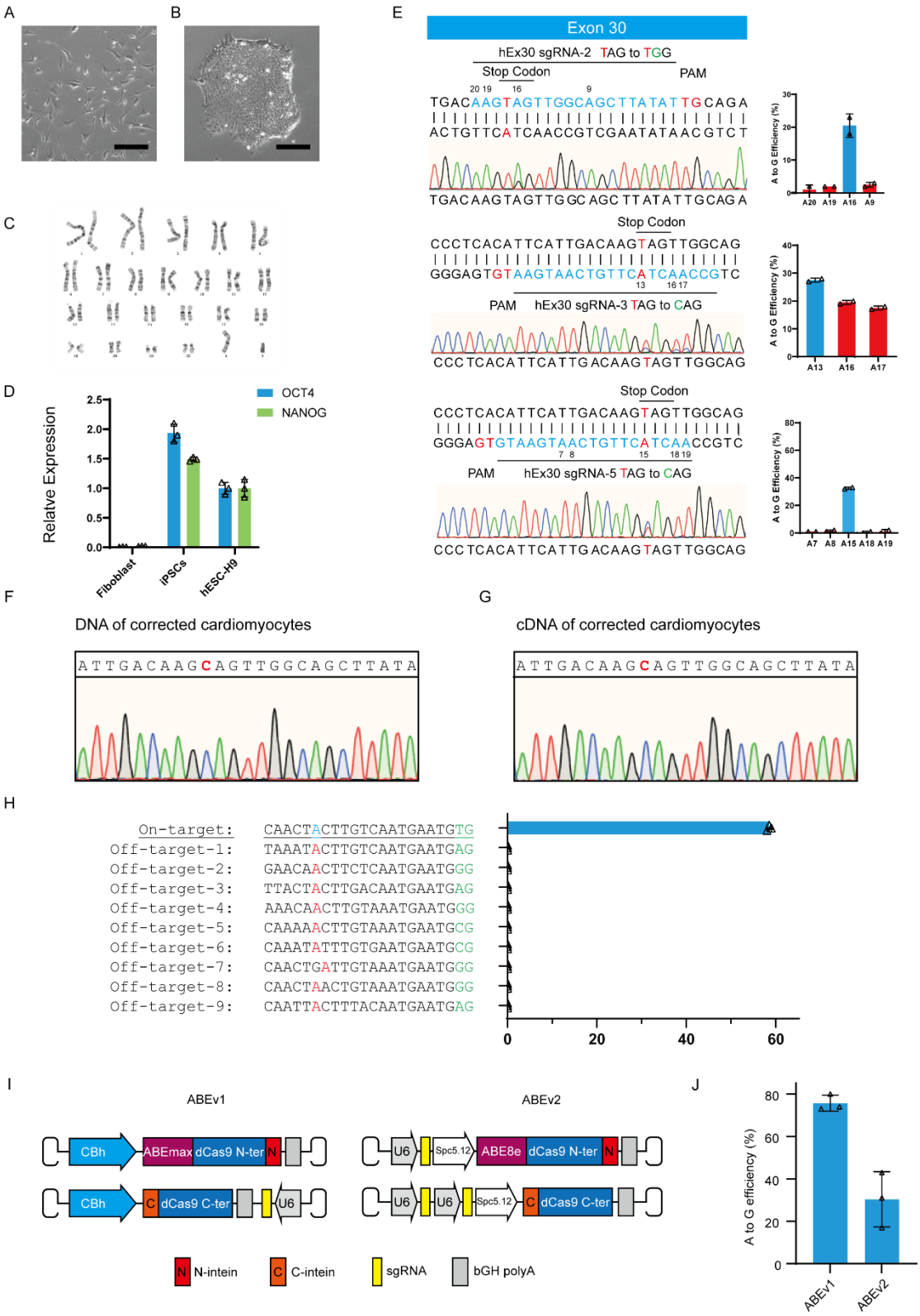

Figure S2. Characterization of human DMD iPSC cells and off-target analysis.

(A) Representive morphology of DMD patient fibroblasts. The image was taken under a light microscope at 10×. **(B)** Representive picture of human DMD iPSC

colony. The picture was conducted with a light microscope at 20×. **(C)** Karyotype analysis of human DMD iPSC cells. **(D)** RT-PCR analyses of pluripotency markers OCT4 and NANOG in human DMD iPSC and normal H9 cells (n=3). DMD patient fibroblast was used as the negative control. **(E) Left**: Schematic for the binding position of hEx30 sgRNA-2, sgRNA-3, or sgRNA-5 in the exon 30 mutant. The PAM and sgRNA sequences are present in red and blue respectively. The adenines are numbered from the PAM. The representative chromatogram of genomic sequencing was performed in human DMD iPSCs. **Right**: The percentages of genomic edits by full-length SpG-ABE and hEx30 sgRNA in human DMD iPSCs (n=3). On-target editing is shown in blue. **(F)** Sanger sequence of corrected cardiomyocyte DNA. (G) Sanger sequence of corrected cardiomyocyte cDNA. **(H)** Deep sequencing analysis of genomic modifications at the on-target and top predicated off-target sites of hEx30 sgRNA-3 (n=3). On-target editing is present in blue. **(I)** Illustration for the intein-mediated split-SpG-ABE systems. The N- and C-terminal ABEs in the ABEv1 or ABEv2 system are driven by the promoter CBh or SPc5-12 respectively, while human sgRNA cassette in both ABEv1 and ABEv2 systems is controlled by the U6 promoter. **(J)** The percentages of DNA edits at the A15 in human DMD iPSCs treated with hEx30 sgRNA-4 and split-SpG-ABE systems (n= 3). Quantitative data are presented as mean ± SEM.

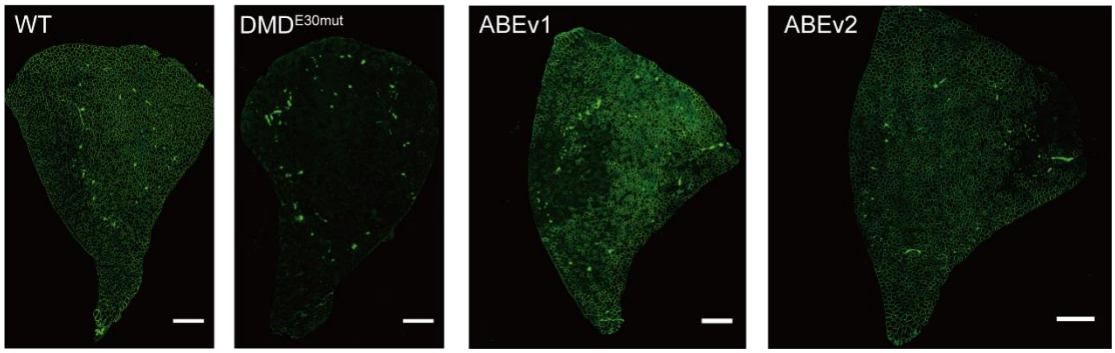

Figure S3. ABE-driven restoration of dystrophin expression in skeletal muscles of adult DMD^{E30mut} mice.

Immunofluorescence analysis of dystrophin protein expression in entire TA muscles of WT mice and DMD^{E30mut} mice with ABE or saline treatment. Dystrophin is present in green. Scale bar, 500 μm.

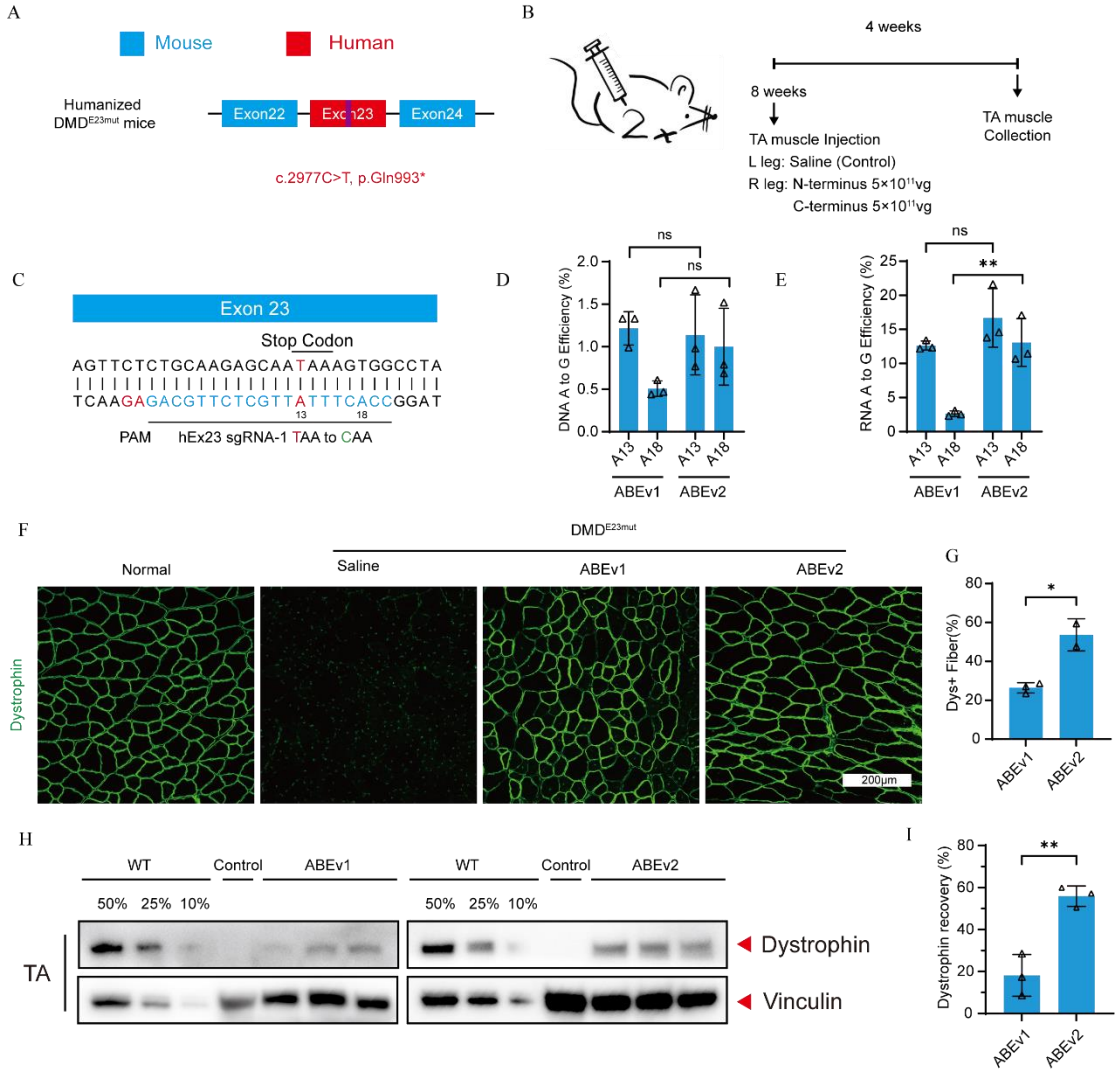

Figure S4. Local ABE delivery rescues dystrophin expression in adult DMD^{E23mut} mice.

(A) Illustration for the nonsense c.2977C>T mutation in human exon 23 sequence of the humanized DMD^{E23mut} mice. **(B)** Illustration for the intramuscular infusion of split-ABE components in 8-week-old humanized DMD^{E23mut} mice. Mouse right TA muscles were infused with N- and C-terminal ABEs by the AAV9 particles at the total dose of 5 × 10^{11} vg/leg, while the left legs receiving saline treatment were the negative controls. **(C)** Schematic for the binding position of hEx23 sgRNA-1 in the exon 23 mutant. The PAM and sgRNA are shown in red and blue respectively. The adenines in the editing window are numbered from the PAM. **(D)** The percentages of genomic editing events in mouse TA muscles with saline or ABE treatment (n=3). **(E)** The

percentages of modification events in the transcripts of mouse TA muscles receiving saline or ABE treatment (n=3). **(F)** Immunohistochemistry of dystrophin expression in the TA muscles of age-matched WT mice and DMD^{E23mut} mice with ABE or saline treatment. Dystrophin is present in green. Scale bar, 200 μm. **(G)** Quantification of dystrophin+ myofibers in the cross-sections of mouse TA muscles with ABE or saline treatment (n=3). **(H)** Western blotting of dystrophin and vinculin proteins in the TA muscles of age-matched WT mice and DMD^{E23mut} mice with ABE or saline treatment. The proteins from WT mice were used to standardize dystrophin expression levels. **(I)** Quantification of dystrophin expression level in ABE-treated DMD^{E23mut} mice after normalization to vinculin expression (n=3). Quantification is shown as mean ± SEM. Each triangle represents an individual mouse. NS, not significant; *P < 0.05; **P < 0.01.

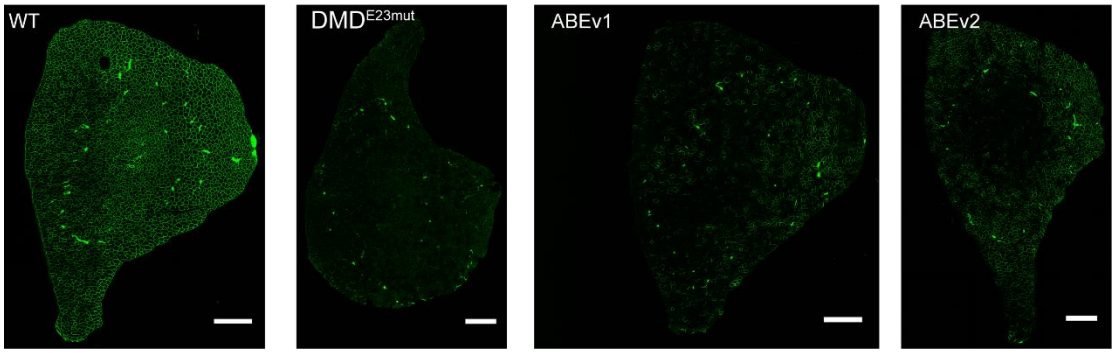

Figure S5. Restoration of dystrophin expression after local ABE infusion in DMD^{E23mut} mice.

Immunohistochemistry of dystrophin expression in entire TA muscles of WT mice and DMD^{E23mut} mice without or with ABE treatment. Dystrophin is shown in green. Scale bar, 500 μm.

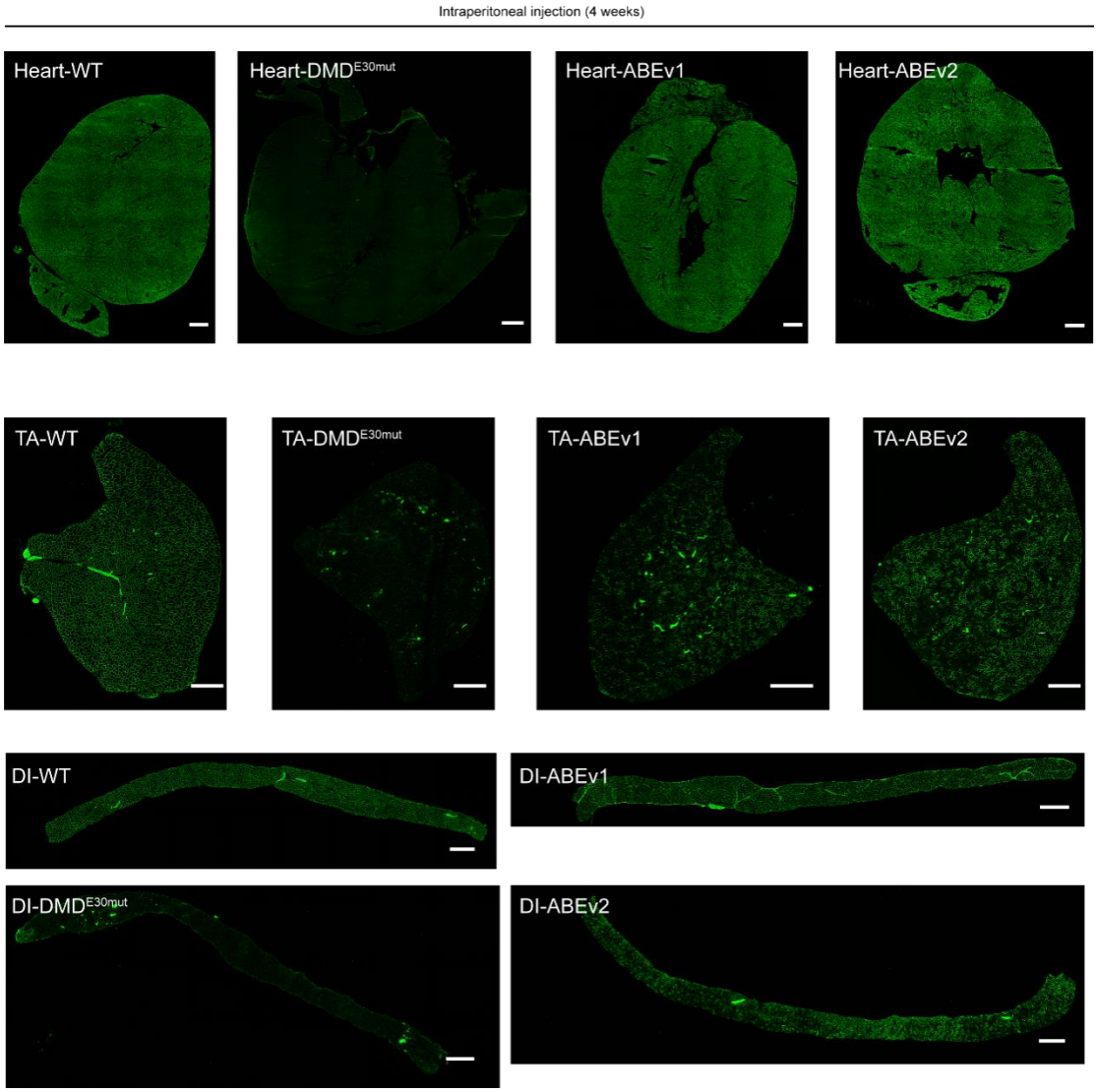

Figure S6. Body-wide dystrophin restoration by systemic ABE administration in neonatal DMD^{E30mut} mice.

Immunohistochemistry of dystrophin protein in entire HE, DI, and TA tissues from WT mice and DMD^{E30mut} mice receiving saline or ABE treatment. Dystrophin is present in green. Scale bar, 500 μm.

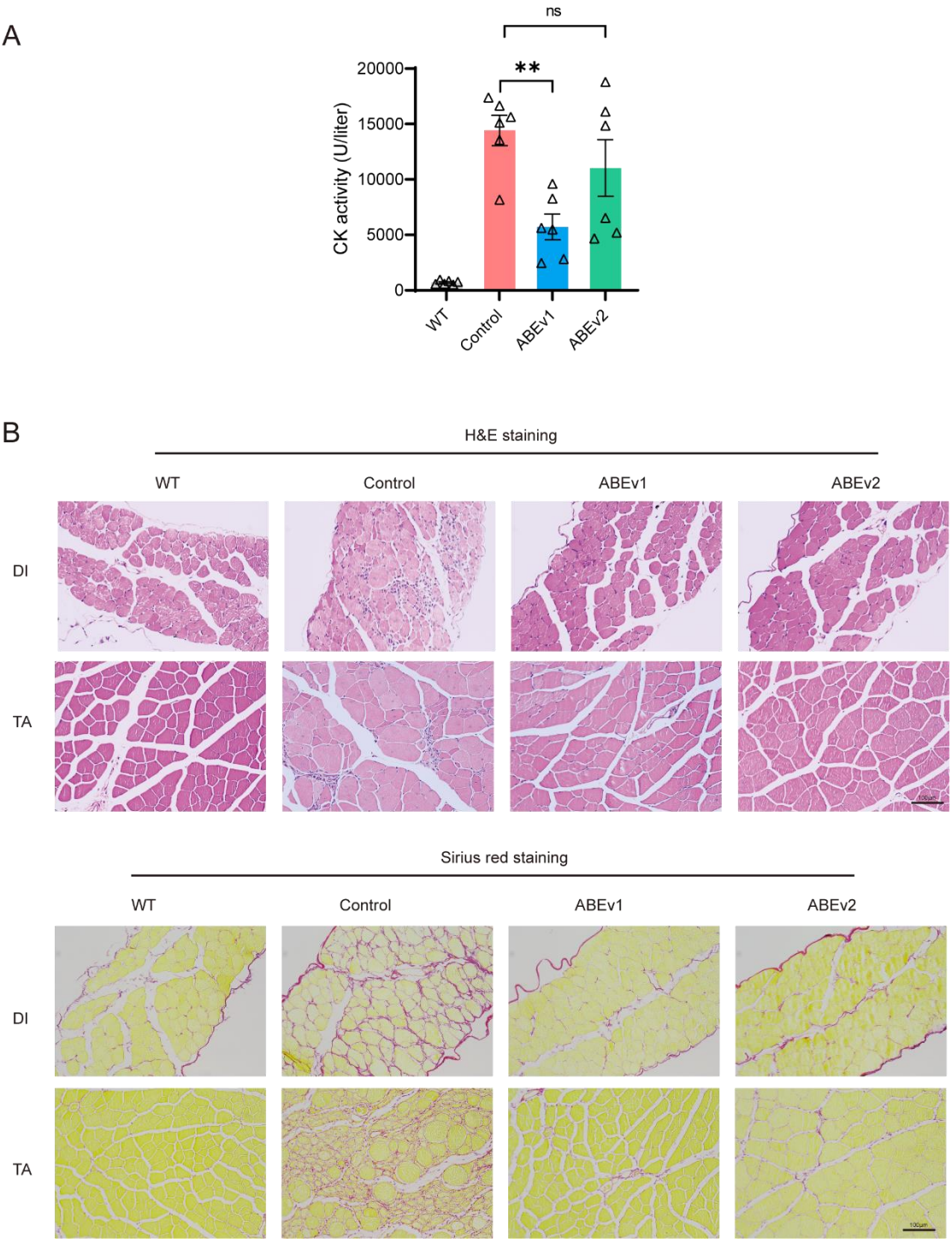

Figure S7. H&E histology staining and CK analysis results after ABE systemic administration. **(A)**Characterization of CK activity after intraperitoneal injection (n=6). Significance is indicated by asterisk and determined using unpaired two-tailed Student's t test. ns represents not statistically significant. **(B)** H&E and Sirius red staining of TA and DI muscle of WT, untreated, and AAV-ABE treated DMD mice. Scale bars, 100μm.

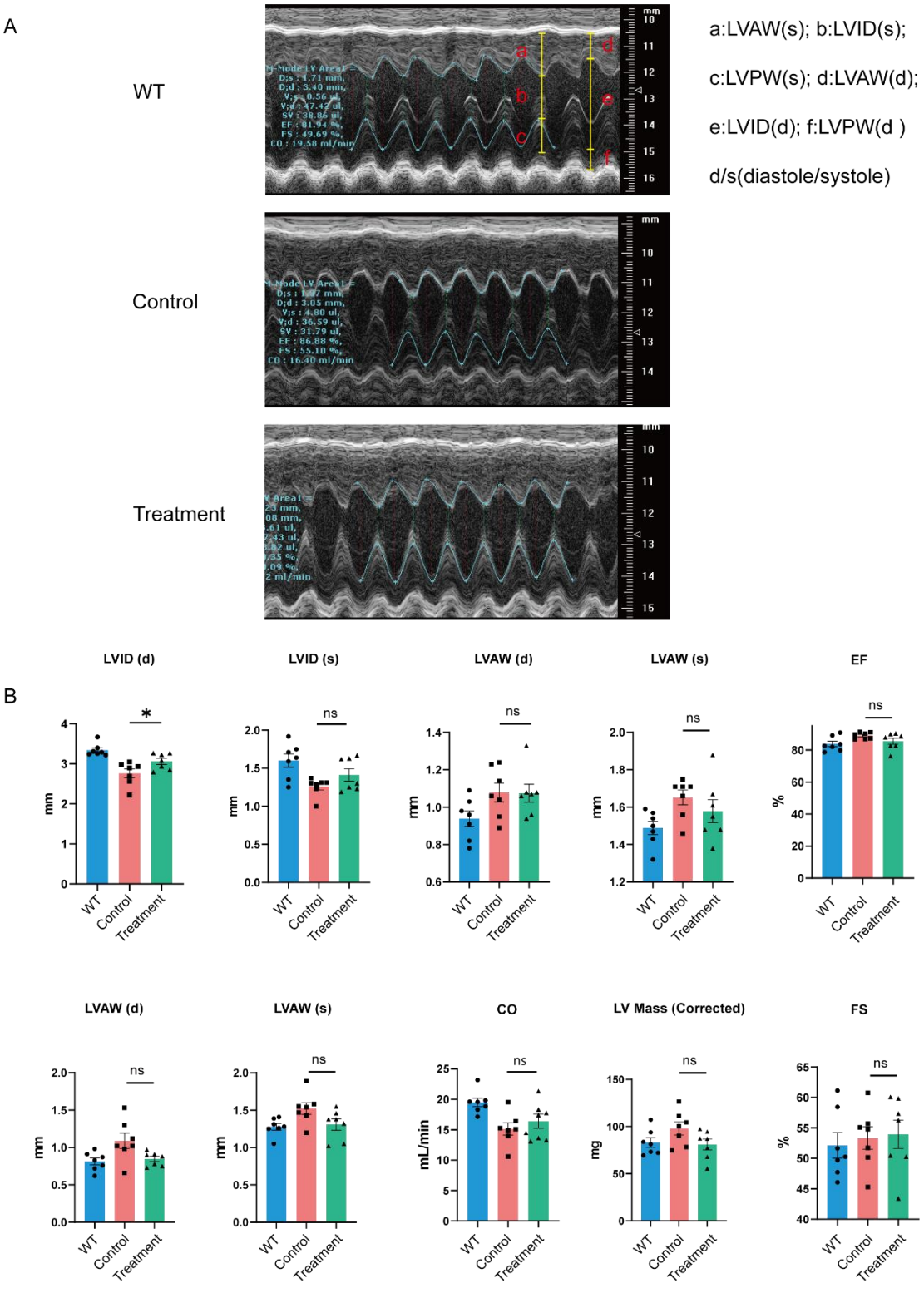

Figure S8. Echocardiography was used to assess the cardiac function of DMD mice after systemic delivery of ABEv2.

(A) Representative echocardiographic image for DMD^{E30mut} mice with or without

ABEv2 administration were monitored for 6 weeks. Age-matched wild-type and DMD mice were included as controls.

(B) Echocardiographic analysis was performed in WT, DMD-mock, and DMD mice treated with ABEv2 after 6 weeks injection. LVID;d or LVID;s: Left Ventricular Internal Diameter during diastole or systole; LVPW;d or LVPW;s: Left Ventricular Posterior Wall Thickness during diastole or systole; LVAW;d or LVAW;s: Left Ventricular Anterior Wall Thickness during diastole or systole; EF: Ejection Fraction; FS: Fractional Shortening; CO: Cardiac Output; LV Mass (corrected): Left Ventricular Mass corrected for body surface area. Values are shown as mean ± SEM. Significance is indicated by asterisk and determined using unpaired two-tailed Student's t test. NS represents not statistically significant.

Table S1. Nonsence mutation of patients in our database

Gender	Diagnose at Age	Diagnosis	Mutant	Codon	Nonsense Mutation
M	3	DMD	E6, c.433 C > T, p.Arg145*	CGA	TGA
M	8	DMD	E23, c.2977C>T, p.Gln993*	CAA	TAA
M	9	DMD	E24, c.3189G>A, p.Trp1063*	TGG	TGA
M	5	DMD	E25, c.3414G>A, p.Trp1138*	TGG	TGA
M	8	DMD	E30, c.4174C>T, p.Gln1392*	CAG	TAG
M	7	DMD	E35, c.4996C>T, p.Arg1666*	CGA	TGA
M	4	DMD	E37, c.5247C>A, p.Cys1749*	TGC	TGA
M	7	DMD	E41, c.5899C>T, p.Arg1967*	CGA	TGA
M	6	DMD	E44, c.6292C>T,p.Arg2098*	CGA	TGA
M	7	DMD	E54, c.8009 A>G, p.Trp2670*	TGG	TAG
M	6	DMD	E55, c.8038C>T,p.Arg2680*	CGA	TGA
M	7	DMD	E56, c.8230G>T, p.Glu2744*	GAA	TAA
M	10	DMD	E59, c.8713C>T,p.Arg2950*	CGA	TGA
M	6	DMD	E34, c.4729C>T， p.Arg768*	CGA	TGA
M	6	DMD	E19, c.2302C>T,p.Arg1577*	CGA	TGA
M	3	DMD	E21,c.2695G>T,p.Glu899*	GAG	TAG
M	10	DMD	E21,c.2776C>T,p.Gln926*	CAG	TAG
M	4	DMD	E20,c.2527G>T,p.Glu843*	GAG	TAG
M	7	DMD	E41,c.5899C>T,p.Arg1967*	CGA	TGA
M	9	DMD	E24,c.3189G>A,p.Trp1063*	TGG	TGA
M	3	DMD	E25,c.3337C>T,p.Gln1113*	CAG	TAG
M	1	DMD	E43,c.6188T>A,p.Leu2063*	TTG	TAG
M	8	DMD	E30,c.4117C>T,p.Gln1373*	CAG	TAG
M	4	DMD	E20,c.2407C>T,p.Gln803*	CAA	TAA
M	10	DMD	E70,c.10141C>T,p.Arg3381*	CGA	TGA
M	6	DMD	E36,c.5125A>T,Lys1709*	AAA	TAA

M	3	DMD	E13,c.1510C>T,p.Gln504*	CAA	TAA

Table S2 Target sgRNA and primer sequence.

Experiment	Primer name	Primer sequence (5'-3')
PCR primer flanking human exon 30	hDMD_420F	CCAGGAAGCTGCGAAATCTG
	hDMD_420R	TCAGTGAATCAAAACAACCCCA
RT-PCR primer flanking human exon 30	RT-hDMD-665F	GCGACATTCAGAGGATAACCC
	RT-hDMD-665R	CTGTACAATCTGACGTCCAGT
qPCR primer of human OCT4	hOCT4_qPCR_f	CAGTGCCCGAAACCCACAC
	hOCT4_qPCR_r	GGAGACCCAGCAGCCTCAAA
qPCR primer of human NANOG	hNANOG_qPCR_f	CAGAAGGCCTCAGCACCTAC
	hNANOG_qPCR_r	ATTGTTCCAGGTCTGGTTGC
Genotyping of DMD^{E30mut} mice	DMD^{E30mut}-2333F	ATTCATATAGGGCTTCAGTTCC
	DMD^{E30mut}-2333R	CATCTGTTTTAATAGTGTGCAT
RT-PCR of DMD^{E30mut} mice	RT-mDMD-358F	AATCAGATTCGTCTATTGGCACA
	RT-mDMD-358R	CCCTTTGGTTGGCATCCTT
Genotyping of DMD^{E23mut} mice	DMD^{E23mut}-2395F	CACTTTACCACCAATGCGCTA
	DMD^{E23mut}-2395R	AAGAAAATGCAAAAGGACCCC
RT-PCR of DMD^{E23mut} mice	RT-mDMD-618F	CACTTTACCACCAATGCGCTA
	RT-mDMD-618R	CGGCATATGTGATCCCACT
DNA base editing sgRNA in *DMD* c.433 C > T	sgRNA1_F	caccgATTGTCaGACCCAGCTCAGG
	sgRNA1_R	aaacCCTGAGCTGGGTCtGACAATc
	sgRNA2_F	caccgTGATTGTCaGACCCAGCTCA
	sgRNA2_R	aaacTGAGCTGGGTCtGACAATCAc
DNA base editing sgRNA in *DMD* c.2977C>T	sgRNA3_F	caccgccactttAttgctcttgcag
	sgRNA3_R	aaacctgcaagagcaaTaaagtggc
	sgRNA4_F	caccggccactttAttgctcttgc
	sgRNA4_R	aaacgcaagagcaaTaaagtggcc
	sgRNA5_F	caccgataggccactttAttgctct
	sgRNA5_R	aaacagagcaaTaaagtggcctatc
DNA base editing sgRNA in DMD c.3189G>A	sgRNA6_F	caccgAAATGAATGGCTGAAGTTGA
	sgRNA6_R	aaacTCAACTTCAGCCATTCATTTc
	sgRNA7_F	caccgAAGAAATGAATGGCTGAAGT
	sgRNA7_R	aaacACTTCAGCCATTCATTTCTTc
	sgRNA8_F	caccgCCATTCATTTCTTCAGGGTT
	sgRNA8_R	aaacAACCCTGAAGAAATGAATGGc
DNA base editing sgRNA in DMD c.3414G>A	sgRNA9_F	caccGTGaGATCACATGTGCCAAC
	sgRNA9_R	aaacGTTGGCACATGTGATCtCAC
	sgRNA10_F	caccgTGTGATCtCACTGAGTGTTA
	sgRNA10_R	aaacTAACACTCAGTGaGATCACAc
	sgRNA11_F	caccgAAGtAGTTGGCAGCTTATAT

DNA base editing sgRNA in DMD c.4174C>T	sgRNA11_R	aaacATATAAGCTGCCAACTaCTTc
	sgRNA12_F	caccgAGtAGTTGGCAGCTTATAT
	sgRNA12_R	aaacATATAAGCTGCCAACTaCTc
	sgRNA13_F	caccGCCAACTaCTTGTCAATGAA
	sgRNA13_R	aaacTTCATTGACAAGtAGTTGGC
	sgRNA14_F	caccgCAACTaCTTGTCAATGAATG
	sgRNA14_R	aaacCATTCATTGACAAGtAGTTGc
	sgRNA15_F	caccgAACTaCTTGTCAATGAATG
	sgRNA15_R	aaacCATTCATTGACAAGtAGTTc
DNA base editing sgRNA in DMD c.4996C>T	sgRNA16_F	caccgTCaGGAGGTGACAGCTATCC
	sgRNA16_R	aaacGGATAGCTGTCACCTCCtGAc
	sgRNA17_F	caccgCACCTCCtGAGCAGAAGAGT
	sgRNA17_R	aaacACTCTTCTGCTCaGGAGGTGc
DNA base editing sgRNA in DMD c.5247C>A	sgRNA18_F	caccgCTtCAGTGGTCACCGCGGTT
	sgRNA18_R	aaacAACCGCGGTGACCACTGaAGc
	sgRNA19_F	caccgCCACTGaAGGAAATTAGTAG
	sgRNA19_R	aaacCTACTAATTTCCTtCAGTGGc
	sgRNA20_F	caccgTTTCCTtCAGTGGTCACCGC
	sgRNA20_R	aaacGCGGTGACCACTGaAGGAAAc
DNA base editing sgRNA in DMD c.5899C>T	sgRNA21_F	caccgTCTTCaAAACTGAGCAAATT
	sgRNA21_R	aaacAATTTGCTCAGTTTtGAAGAc
	sgRNA22_F	caccgCAGTTTtGAAGACTCAACTT
	sgRNA22_R	aaacAAGTTGAGTCTTCaAAACTGc
DNA base editing sgRNA in DMD c.6292C>T	sgRNA23_F	caccgAAATCACCCTTGTCGGTCCT
	sgRNA23_R	aaacAGGACCGACAAGGGTGATTTc
	sgRNA24_F	caccGGGTGATTTGACAGATCTGT
	sgRNA24_R	aaacACAGATCTGTCAAATCACCC
	sgRNA25_F	caccgCAAGGGTGATTTGACAGATC
	sgRNA25_R	aaacGATCTGTCAAATCACCCTTGc
DNA base editing sgRNA in DMD c.8009A>G	sgRNA26_F	caccgctTagagaagcattcataaa
	sgRNA26_R	aaactggatctttttctAAggttc
	sgRNA27_F	caccgtTagagaagcattcataaaa
	sgRNA27_R	aaacttttatgaatgcttctctAac
	sgRNA28_F	caccgaatgcttctctAagaggcat
	sgRNA28_R	aaacatgcctctTagagaagcattc
DNA base editing sgRNA in DMD c.8038C>T	sgRNA29_F	caccGAGTGAGAGGCTGCTTTGGA
	sgRNA29_R	aaacTCCAAAGCAGCCTCTCACTC
	sgRNA30_F	caccgAGTGAGTGAGAGGCTGCTTT
	sgRNA30_R	aaacAAAGCAGCCTCTCACTCACTc
	sgRNA31_F	caccgCTCACTCACTCACCCTTTTA
	sgRNA31_R	aaacTAAAAGGGTGAGTGAGTGAGc
DNA base editing sgRNA in DMD c.8713C>T	sgRNA32_F	caccgCTGCTTTCATAGAAGCCGAG
	sgRNA32_R	aaacCTCGGCTTCTATGAAAGCAGc

	sgRNA33_F	caccgCTATGAAAGCAGGCTGAGGA
	sgRNA33_R	aaacTCCTCAGCCTGCTTTCATAGc